Chinese Chemical Letters 37 (2026) 111447

Contents lists available at ScienceDirect

Chinese Chemical Letters

journal homepage: www.elsevier.com/locate/cclet

A coacervate-based redox-responsive cytoplasmic delivery system for antioxidant macromolecule to rescue sensorineural hearing loss

Penghui Chen[a,d,e,1], Jianmian Fu[b,1], Shule Hou[a,d,e,1], Jifang Zhang[a,d,e], Tianyu Gong[a,d,e], Jingyi Zhu[a,d,e], Sihan Huang[a,d,e], Yuxuan Wu[a,d,e], Qing Zhang[a,d,e], Maoli Duan[g,h], Jiarui Chen[f,*], Jin Xie[a,d,e,*], Yangyang Yang[b,*], Jun Yang[a,d,e,*], Xuhong Qian[b,c]

[a] *Department of Otorhinolaryngology-Head and Neck Surgery, Xinhua Hospital, Shanghai Jiao Tong University School of Medicine, Shanghai 200082, China*
[b] *Shanghai Key Laboratory of Chemical Biology, School of Pharmacy, East China University of Science and Technology, Shanghai 200237, China*
[c] *State Key Laboratory of Bioreactor Engineering, East China University of Science and Technology, Shanghai 200237, China*
[d] *Ear Institute, Shanghai Jiao Tong University School of Medicine, Shanghai 200082, China*
[e] *Shanghai Key Laboratory of Translational Medicine on Ear and Nose Diseases, Shanghai 200082, China*
[f] *Department of Otolaryngology-Head and Neck Surgery, Shanghai Children's Hospital, School of Medicine, Shanghai Jiao Tong University, Shanghai 200127, China*
[g] *Ear Nose and Throat Patient Area, Trauma and Reparative Medicine Theme, Karolinska University Hospital, Stockholm 17717, Sweden*
[h] *Division of Ear, Nose and Throat Diseases, Department of Clinical Science, Intervention and Technology, Karolinska Institute, Stockholm 17717, Sweden*

ARTICLE INFO

Article history:
Received 22 March 2025
Revised 9 June 2025
Accepted 10 June 2025
Available online 11 June 2025

Keywords:
Coacervate microdroplets
Redox-responsive release
Targeted intracellular delivery
Sensorineural hearing loss
Antioxidant therapy

ABSTRACT

Sensorineural hearing loss (SNHL) is a prevalent global health issue, primarily caused by excessive generation of reactive oxygen species (ROS) due to acoustic trauma, aging, and ototoxic drugs. Natural antioxidant enzymes, such as catalase (CAT), possess remarkable ROS scavenging capabilities and hold significant potential for SNHL treatment. However, their clinical application is hindered by inefficient delivery and limited stability. Here, we introduce a novel peptide-oligosaccharide conjugate, sELP-ON, which forms coacervate microdroplets *via* liquid–liquid phase separation. These microdroplets efficiently encapsulate and stably carry CAT, releasing it in a glutathione-triggered, redox-responsive manner. The CAT-loaded sELP-ON (sELP-ON@CAT) enhanced cellular uptake through direct cytoplasmic internalization and demonstrates a more robust ROS scavenging activity than naked CAT treatment. Local administration of sELP-ON@CAT in an acoustic injury mouse model effectively rescues hearing loss by reducing cochlear ROS levels, thereby mitigating hair cell loss, ribbon synapse depletion, stria vascularis shrinkage and spiral ganglion neuron degeneration. In summary, our innovative coacervate microdroplet system enables targeted, redox-responsive cytoplasmic delivery of macromolecular antioxidants, offering a novel and effective strategy for treating SNHL.

© 2026 Published by Elsevier B.V. on behalf of Chinese Chemical Society and Institute of Materia Medica, Chinese Academy of Medical Sciences.

Sensorineural hearing loss (SNHL), the most common sensory disorder in human, which is expected to affect over 10% of the global population by 2050, has become a major public health challenge [1]. The etiology of SNHL is multifactorial, primarily attributed to acoustic trauma, aging and ototoxic drugs [2–4]. The pathogenic mechanisms of SNHL are complex, involving multiple biologic and physiologic processes [5,6]. It has been demonstrated that excessive reactive oxygen species (ROS) generation due to various factors such as acoustic trauma, ototoxic drugs and aging, can trigger inflammatory reactions that harm cochlear hair cells (HCs) and neurons, as well as result in cell death and accelerating hearing loss [7–9]. Extensive investigations in animal models identified various antioxidants that neutralize excessive intracellular ROS—efficiently combating ROS-mediated pathologies, including SNHL. Among these, ROS-scavenging enzymes, like catalase (CAT) and superoxide dismutase (SOD), are highly promising due to their exceptional bioactivity and biocompatibility for *in vitro* applications [10–14]. Yet, the implementation of these natural enzymes has encountered several challenges due to their limited stability, high sensitivity to fabrication and stocking requirements, and short half-life [15]. In addition, their large molecular size hampers direct penetration into the cytoplasm to react with intracellular ROS [16–18].

* Corresponding authors.
E-mail addresses: drchenjiarui@163.com (J. Chen), xjmdsh@163.com (J. Xie), triyang@ecust.edu.cn (Y. Yang), yangjun@xinhuamed.com.cn (J. Yang).
[1] These authors contributed equally to this work.

https://doi.org/10.1016/j.cclet.2025.111447
1001-8417/© 2026 Published by Elsevier B.V. on behalf of Chinese Chemical Society and Institute of Materia Medica, Chinese Academy of Medical Sciences.

To overcome these limitations, researchers are actively working on designing and developing enzyme-based biomaterials. Natural enzymes can be either integrated into different types of carriers such as polymers, nanomaterials or biomaterials by encapsulation, copolymerisation and surface immobilisation methods [19–22]. Although various delivery systems have been developed to address these challenges, the current reliance on nanoformulations to penetrate cell membranes *via* endocytosis limits cytoplasmic release of active ingredients, reducing efficacy and delivery efficiency [23–26]. Therefore, developing an efficient system to directly deliver ROS-scavenging enzymes into cochlear HCs and release them in the cytoplasm remains an unmet need.

Current therapeutic delivery systems, especially for protein-based drugs, still face several limitations. For instance, polymeric materials often present challenges in synthesis and preparation [27,28]. Similarly, lipid nanoparticles (LNPs) exhibit complex compositions and are limited in protein encapsulation and immunogenicity concerns [29–31]. Therefore, new efficient delivery systems are needed for protein delivery. Coacervates, formed through liquid–liquid phase separation (LLPS), have garnered attention due to their biomimetic properties that mimic cellular environments. These coacervates are capable of sequestering molecules of varying sizes or charges due to their membraneless nature, offering effectively encapsulating biomolecules without the need for complex modifications. Additionally, coacervates can be engineered to exhibit specific membrane-penetrating behaviors, enabling the direct delivery of therapeutic agents into the cytosol [28,32]. This membrane-penetrating ability provides distinct advantages for the targeted delivery of therapeutic biomolecules [33–40]. Thus, coacervate is considered as a promising carrier for delivering therapeutic biomolecules, with the added benefit of specific membrane-penetrating behavior enabling direct cytosolic delivery. Accordingly, coacervate is postulated suitable for delivering ROS-scavenging enzymes to treat SNHL, a novel delivery strategy yet to be explored.

We have developed a series of short elastin-like polypeptide–oligonucleotide conjugates (sELP-ONs) that undergo temperature-responsive LLPS to form coacervates [41]. These sELP-ON coacervates have shown exceptional ability to encapsulate various biomolecules, including proteins with different charges and molecular weights, highlighting their potential as versatile delivery platforms for the treatment of SNHL. Herein, we rationally designed a new sELP-ON coacervate incorporating disulfide bonds as redox-responsive linkers, enabling glutathione-triggered disassembly within the intracellular environment.

Furthermore, CAT-an enzyme with ROS-scavenging activity-was loaded into the sELP-ON coacervates (sELP-ON@CAT). These coacervates are expected to deliver CAT directly into cochlear HC cytoplasm, where glutathione-triggered disulfide reduction will induce coacervate disassembly and responsive release of CAT, ultimately resulting in ROS scavenging and promoting auditory recovery in SNHL induced by acoustic trauma. Therefore, the sELP-ON coacervates not only protect CAT from external environmental influences but also enable CAT release spontaneously under specific ROS conditions to achieve therapeutic effects.

Monomer sELP-ON was synthesized by conjugating sELP ($[VPGFG]_6$]C) with single-stranded oligonucleotide *via* disulfide bond formation through three-step reactions (Fig. 1A and Fig. S1 in Supporting information). The final products were confirmed using high-performance liquid chromatography and polyacrylamide gel electrophoresis (PAGE) (Fig. S2 in Supporting information). In addition, sELP-ON reducing agents—such as glutathione, abundant in cells—are widely used as efficient stimuli for the redox-responsive release of encapsulated drugs in nano- and micro-delivery system [42]. The disassembly of sELP-ON conjugates in response to the presence of glutathione was verified using 10 % PAGE (Fig. S3 in Supporting information).

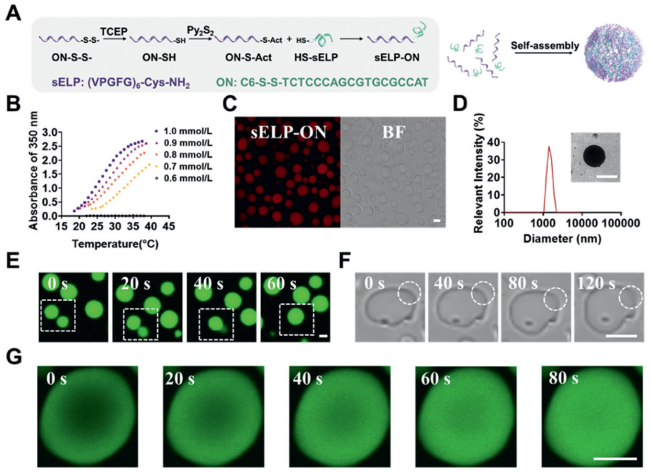


Fig. 1. Self-assembly and characterization of sELP-ON microdroplets. (A) Construction and self-assembly of sELP-ON conjugates. (B) Turbidity profiles of absorbance at 350 nm for sELP-ON at different concentrations. (C) Confocal images of TAMRA-labeled sELP-ON microdroplets (1 mmol/L). (D) DLS analysis and TEM images of sELP-ON (1 mmol/L). (E) Time-lapse images of fusion in sELP-ON microdroplets (1 mmol/L) stained with FITC. (F) Time-lapse images of the wetting of a glass substrate with sELP-ON microdroplets (1 mmol/L). (G) Time-lapse images of FRAP in a single sELP-ON droplet stained with FITC. Scale bar: 2 μm.

Subsequently, the LLPS behaviors of sELP-ON were investigated. Turbidity testing is a canonical method for assessing phase transitions of temperature-responsive materials [43,44], which was employed in this study. The transition temperature (T_t) of sELP-ON at different concentrations was determined by monitoring absorbance changes at 350 nm during cooling. T_t decreased as the sELP-ON concentration increased, with a T_t of 27.5 °C observed for 1 mmol/L sELP-ON solutions, which is ideal for potential *in vivo* enzyme delivery (Fig. 1B). Bright-field and fluorescent images obtained using confocal laser scanning microscopy (CLSM) revealed the formation of micron-sized (~2 μm) spherical particles (Fig. 1C), which were further confirmed by dynamic light scattering (DLS) and transmission electron microscopy (TEM) (Fig. 1D, Fig. S4 in Supporting information). Time-lapse CLSM images showed dynamic fusion behavior (Fig. 1E) and wetting behavior (Fig. 1F), indicating that the microparticles exist in a droplet state. Fluorescence recovery after photobleaching experiments revealed rapid fluorescence recovery within the droplets, confirming the liquid-like properties of sELP-ON coacervate microdroplets (Fig. 1G).

CAT encapsulation in sELP-ON coacervates was achieved by directly adding CAT to sELP-ON coacervate solutions. Fig. 2A shows CLSM images of fluorescein isothiocyanate (FITC)-labeled CAT successfully partitioned into TAMRA-labeled coacervate microdroplets, with an encapsulation efficiency (EE) of approximately 76 %, although the detailed encapsulation mechanism remained unknown. We further characterized the microdroplets encapsulating CAT through DLS and zeta potential measurements. DLS results showed a slight increase in the diameter of the microdroplets after CAT encapsulation (Fig. S5A in Supporting information). We also measured the zeta potential of sELP-ON, CAT, and sELP-ON@CAT, which were −31.49, −46.04, and −38.87, respectively (Fig. S5B in Supporting information). The observed changes in particle size and zeta potential indicate the successful encapsulation of CAT. Additionally, we conducted another experiment to observe the disassembly of microdroplets in the presence of glutathione (GSH). CLSM images were taken to monitor the disassembly of sELP-ON@CAT microdroplets before and after the GSH addition, demonstrating the redox-reponsive releasement property of this system (Fig. S5C

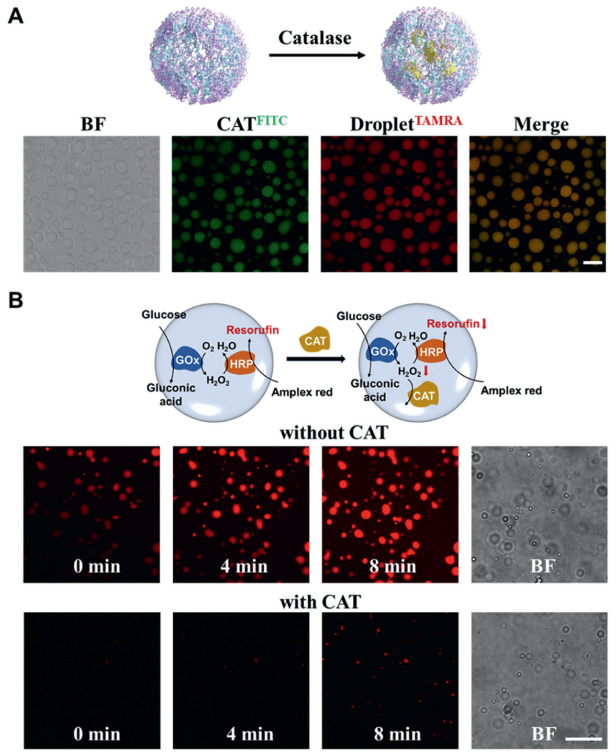


Fig. 2. *In vitro* scavenging of H_2O_2 by sELP-ON@CAT (A) confocal images of TAMRA-labeled sELP-ON microdroplets encapsulating FITC-labeled CAT. (B) Time-lapse images of the GOx/HRP cascade reaction in CAT-encapsulated sELP-ON and control sELP-ON microdroplets lacking CAT. H_2O_2 was detected using the Amplex Red fluorescent probe. sELP-ON concentration: 1 mmol/L. Scale bar: 5 μm.

in Supporting information). To evaluate the ROS-scavenging ability of CAT@sELP-ON coacervates, a glucose oxidase/horseradish peroxidase (GOx/HRP) cascade reaction was incorporated into the coacervate system.

Glucose freely passes through the microdroplets and is oxidized by GOx to form H_2O_2. With HRP, Amplex Red reacts with H_2O_2 to form resorufin, a red fluorescent oxidation product [45,46]. The GOx/HRP-catalyzed reaction was conducted within the sELP-ON compartments. Microdroplets were pre-encapsulated with GOx, HRP, and the reactive oxygen probe Amplex Red, after which glucose was added to the system for real-time fluorescence imaging using CLSM.

Fig. 2B shows that red fluorescence gradually increased inside the microdroplets after adding the control group, indicating a successful GOx/HRP cascade reaction and resorufin generation. In contrast, fluorescence in the CAT–pre-encapsulated group was significantly lower than that in the control group, suggesting that H_2O_2 induce coacervate disassembly and responsive release of CAT, and CAT efficiently consumed H_2O_2, blocking the HRP-mediated reaction and producing fewer fluorescent molecules. Intracellular H_2O_2 levels were measured using the live-cell H_2O_2 probe, MitoSOX (λ_{ex}: 510 nm, λ_{em}: 580 nm; Fig. S6A in Supporting information). Cells treated with H_2O_2 exhibited the highest MitoSOX fluorescence, indicating elevated intracellular H_2O_2 levels. Naked CAT treatment caused a partial reduction in MitoSOX fluorescence, whereas CAT@sELP-ON coacervates significantly decreased MitoSOX fluorescence, demonstrating effective H_2O_2 scavenging owing to CAT delivery (Fig. S6B in Supporting information). sELP-ON coacervates will potentially facilitate intracellular delivery of CAT, mitigating ROS-induced damage, scavenging ROS, and restoring cell viability *via* CAT-mediated intracellular H_2O_2 catabolism [47–49]. Cell counting kit-8 (CCK8) experiments showed that sELP-ON coacervates exhibit no cytotoxicity while counteracting H_2O_2-induced cytotoxicity in HEI-OC1 cells (Fig. S6C in Supporting information). Internalization of sELP-ON coacervates was assessed by incubating FITC-labeled sELP-ON coacervates with HeLa cells for 6, 12, 18, and 24 h and visualizing the results using CLSM. Notable internalization started at 18 h, peaking at 24 h (Fig. S7A in Supporting information); thus, 24-h incubation of sELP-ON coacervates was used for subsequent experiments. As Rhodamine B isothiocyanate (RBITC)-labeled CAT and FITC-labeled sELP-ON coacervate microdroplets exhibited remarkable colocalization (Pearson's correlation coefficient = 0.807), indicating successful cytoplasmic delivery of CAT, delivery of CAT into the cytoplasm was confirmed (Fig. S7B in Supporting information).

To confirm the internalization pathway of sELP-ON coacervates, HEI-OC1 cells were treated with four endocytosis inhibitors: the clathrin-mediated endocytosis inhibitor chlorpromazine (CPZ), pinocytosis inhibitor amiloride (AML), energy-dependent endocytosis inhibitor sodium azide (NaN_3), and lipid raft-mediated pathway inhibitor methyl-β-cyclodextrin (MβCD) [50–53]. AML pretreatment exerted a minimal effect on cellular uptake of sELP-ON coacervates. Similarly, CPZ and NaN_3 pretreatment did not significantly affect internalization. However, MβCD pretreatment remarkably inhibited coacervate internalization (Fig. S8A in Supporting information). Mean fluorescence intensity measurements corroborated these results (Fig. S8B in Supporting information). Results for MβCD—which interferes with cholesterol synthesis and inhibits caveolin function—indicate the critical role of cholesterol-dependent lipid rafts in the internalization of sELP-ON coacervates (Fig. S8C in Supporting information); this aligns with findings from other studies of complex coacervates containing oligoarginines, in which interactions with lipid membranes and subsequent lipid sequestration were crucial for membrane penetration [34]. However, it is quite challenging to directly observe this lipid raft-mediated internalization pathway under this experimental condition. Moreover, sELP-ON coacervates, akin to oligoarginine-based coacervates, considerably rely on specific lipid interactions rather than classical endocytic pathways, such as clathrin-mediated endocytosis, for uptake. This process involves cell membrane rearrangement, facilitating direct delivery and release of biomacromolecules into the cytosol while preserving their bioactivity.

Noise induced hearing loss (NIHL) is one of the main types of SNHL, affecting approximately 5 % of the world's population [54]. Following the successful demonstration of biosafety and *in vitro* ROS-scavenging capability of sELP-ON@CAT, the therapeutic potential was investigated in a NIHL mouse mode [55]. All animal procedures have been approved by the Ethics Committee of Xinhua Hospital Affiliated to Shanghai Jiao Tong University School of Medicine (approval No. XHEC–NSFC-2022–198). Fig. 3A illustrates the main procedures of the animal experiments. C57/B6j mice were exposed to 120 dB sound pressure level (SPL) white noise (2–20 kHz for 2 h), creating a permanent NIHL model. To assess treatment efficacy, 2 μL of sELP-ON@CAT was injected into the left inner ear through the round window membrane (RWM) (Fig. 3B) 2 days before noise exposure (−D2) [56], whereas the right ear received 2 μL of phosphate-buffered saline (PBS) as the untreated control. After injection of sELP-ON@CAT, *in vivo* fluorescence imaging was performed for 10 consecutive days. It was found that the ICG fluorescence signal was almost undetectable in the control group. However, the fluorescent signal of sELP-ON@CAT in the left ear was present for >7 days and showed a slow decreasing trend, which indicated the successful delivery of sELP-ON@CAT in the inner ear (Figs. 3C and D). At D3, auditory brainstem response (ABR) thresholds in the treated left ear at click, 4, 8, 16, 24, and 32 kHz were 61.00 ± 6.24, 68.00 ± 13.12, 48.00 ± 8.50, 48.00 ± 8.49, 68.00 ± 18.40, and 66.00 ± 22.48 dB SPL, respectively (Fig. 3E-iv). Moreover, from D7 to D14, hearing improvement in the treated ear

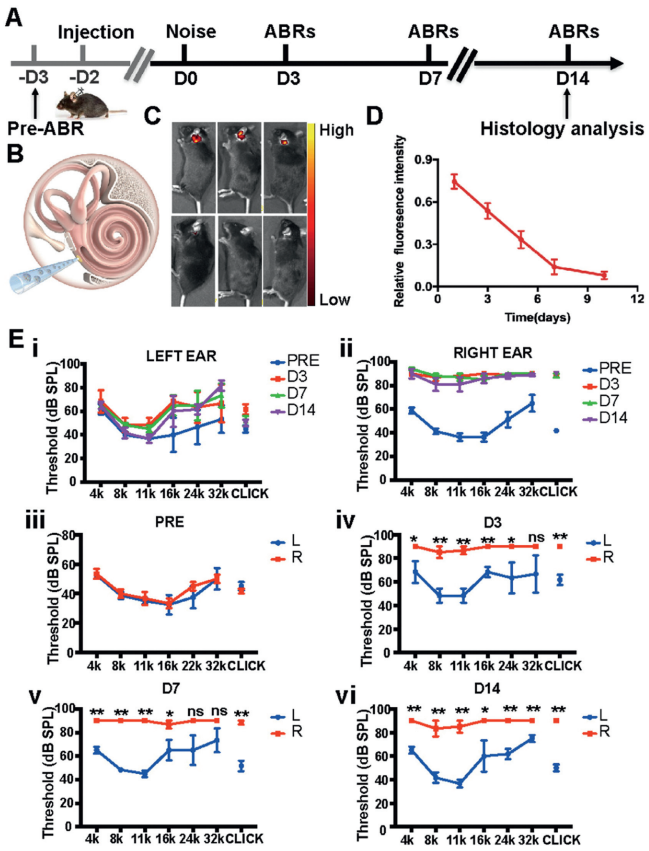


Fig. 3. *In vivo* evaluation of therapeutic efficacy of sELP-ON@CAT in hearing loss therapy. (A) schematic of animal experiments. (B) Mouse round window membrane microinjection pattern diagram. (C) IVIS images of sELP-ON@ICG at different time points within the cochlea on days 1, 3, 5, 7, and 10. (D) Relative fluorescence intensity changes of ICG in IVIS images. (E) ABR thresholds for each group: (i) Hearing threshold changes in the left ear (sELP-ON@CAT-injected: experimental group) before noise exposure (blue line, PRE) and on days 3 (red line, D3), 7 (green line, D7), and 14 (purple line, D14) after exposure. (ii) Hearing threshold changes in the right ear (PBS-injected ear: control group). (iii) Hearing levels in both ears before noise exposure: L (left ear, blue line) and R (right ear, red line). Hearing levels in both ears on (iv) D3, (v) D7, and (vi) D14 following noise exposure. Data are presented as mean ± standard deviation (SD) ($n = 6$). $^{*}P < 0.05$, $^{**}P < 0.01$.

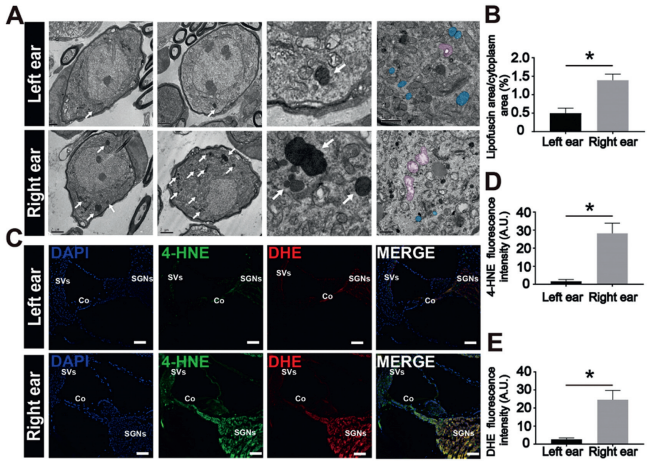


Fig. 4. sELP-ON@CAT mitigates cochlear oxidative stress damage. (A) TEM images of cochlear SGNs showing lipofuscin (white arrows) and mitochondria (blue pseudocolor: normal mitochondria. Pink pseudocolor: swollen mitochondria). Scale bar: 2 μm. (B) 4-HNE and DHE staining to visualize cochlear ROS production. 4-HNE (green), DHE (red), and DAPI (blue). Scale bar: 200 μm. (C–E) Statistical analysis of cytoplasmic lipofuscin percentage and 4-HNE and DHE fluorescence intensity. Data are presented as mean ± SD ($n = 3$). $^{*}P < 0.05$.

continued compared with the untreated ear (Figs. 3E-v and vi). By D14, ABR thresholds at 4, 8, and 11 kHz frequencies in the treated ear had completely recovered to prenoise exposure levels (Fig. 3E-i). In contrast, the untreated right ear exhibited a permanent ABR threshold shift (Fig. 3E-ii). These auditory outcomes suggest that sELP-ON@CAT effectively promotes hearing recovery in NIHL. Cochlear morphology findings suggest that sELP-ON@CAT significantly reduces damage to ribbon synapses, SGNs, nerve fibers, and the SV caused by acoustic trauma (Fig. S9 in Supporting information).

Oxidative stress is a key mechanism in NIHL [57–62]. To assess whether sELP-ON@CAT reduces ROS levels associated with NIHL, several methods were employed to measure these levels in the cochlea. Lipofuscin, a byproduct of unsaturated fat peroxidation found in organelle fragments, appears as a brown pigment in the cytoplasm of parenchymal cells [63]. sELP-ON@CAT administration significantly reduced lipofuscin content in the SGNs of the left ear, as observed *via* TEM (Figs. 4A and C). 4-Hydroxynonenal (4-HNE) [64], a well-known marker of lipid peroxidation and oxidative stress, was also assessed. Dihydroethylene (DHE) [65], a probe for superoxide anions that forms ethidium bromide upon reaction with intracellular superoxide anions, was used to detect superoxide levels. Lower levels of 4-HNE and DHE immunoreactivity were observed in the SV, Corti's organ, and SGNs of treated ears (Figs. 4B, D, and E), indicating that sELP-ON@CAT RWM administered *via* RWM effectively alleviates ROS overload in the cochlea caused by noise overexposure. The observed hearing recovery supports the conclusion that the phase-separated peptide–oligonucleotide conjugates successfully deliver the antioxidant enzyme CAT into cochlear sensory cells *via* direct cytosolic delivery. Overall, noise exposure triggers intracellular glutathione for reducing disulfide bonds in peptide–oligonucleotide conjugates, leading to coacervate disassembly and responsive release of CAT in the inner ear. This process helps scavenge excess ROS, repair damaged cochlear cells, and promote hearing recovery in NIHL.

SNHL is a widespread global health issue, often resulting from excessive ROS generation caused by factors such as acoustic trauma, aging, and ototoxic drugs, for which there is a lack of effective treatment. In search of effective treatments, several innovative strategies have been investigated [66,67]. One such approach is the development of a novel peptide-oligosaccharide conjugate, sELP-ON, which forms coacervate microdroplets through liquid-liquid phase separation. These microdroplets are capable of encapsulating CAT, stabilizing it, and releasing it in a glutathione-triggered, redox-responsive manner. In this study, the sELP-ON@CAT coacervates exhibited excellent biocompatibility, with no cytotoxicity observed and the ability to counteract H_2O_2-induced cytotoxicity. This safety profile is crucial for clinical applications. CLSM confirmed the successful intracellular delivery of CAT, demonstrating the coacervates' ability to penetrate cell membranes. Further investigation into the uptake mechanism revealed that sELP-ON coacervates rely on cholesterol-dependent lipid rafts rather than classical endocytic pathways, such as clathrin-mediated endocytosis, for internalization. This unique mechanism involves cell membrane rearrangement, facilitating direct delivery and release of biomacromolecules into the cytosol while preserving their bioactivity.

The elevation of ROS is a key signaling event in SNHL, indicating that regulating ROS levels in cochlear cells may offer a promising therapeutic strategy for treating SNHL. Our findings suggest that sELP-ON@CAT exerts a protective effect on the auditory system *in vivo* and mitigates the progression of NIHL, presenting it as a potential candidate for the treatment of SNHL. The sELP-ON@CAT possesses crucial advantages for the treatment of SNHL, including

an outstanding loading capacity of CAT, direct cytoplasmic delivery upon specific intracellular stimuli, thereby enabling highly efficient ROS scavenging and alleviating intracellular oxidative stress. However, the exact intracellular ROS scavenging efficiency of CAT after cytoplasmic delivery and detailed mechanism of how reduced ROS protect cochlear hair cell remain unknown.

Despite these promising results, several challenges remain to be addressed for the clinical translation of sELP-ON@CAT. Future research must focus on confirming its therapeutic efficacy following the onset of NIHL, as our current findings are based on pre-exposure administration. Additionally, the development of non-invasive delivery methods is crucial, as the current approach of delivering sELP-ON@CAT *via* the RWM is invasive. Investigating systemic routes of administration, such as intravenous or intratympanic injection, would be essential for practical clinical use. In addition, regulating droplet size remains a key challenge, as current variability leads to inconsistent drug loading. Enhancing droplet uniformity would allow for more precise control over drug release, thereby improving both therapeutic efficacy and safety. In conclusion, while sELP-ON@CAT represents a significant advancement in the treatment of SNHL, further research is needed to overcome these challenges and fully realize its potential in clinical settings.

Declaration of competing interest

The authors declare that they have no known competing financial interests or personal relationships that could have appeared to influence the work reported in this paper.

CRediT authorship contribution statement

Penghui Chen: Writing – review & editing, Writing – original draft, Project administration, Investigation, Funding acquisition, Data curation. **Jianmian Fu:** Writing – review & editing, Writing – original draft, Visualization, Validation, Software, Project administration, Methodology, Investigation, Formal analysis, Data curation, Conceptualization. **Shule Hou:** Writing – review & editing, Writing – original draft, Validation, Project administration, Methodology, Investigation, Funding acquisition, Formal analysis, Data curation. **Jifang Zhang:** Validation, Investigation, Formal analysis. **Tianyu Gong:** Validation, Investigation, Formal analysis. **Jingyi Zhu:** Validation, Investigation, Formal analysis. **Sihan Huang:** Validation, Investigation, Formal analysis. **Yuxuan Wu:** Validation, Investigation, Formal analysis. **Qing Zhang:** Validation, Investigation, Formal analysis. **Maoli Duan:** Validation, Investigation, Formal analysis. **Jiarui Chen:** Validation, Investigation, Formal analysis. **Jin Xie:** Validation, Investigation, Formal analysis. **Yangyang Yang:** Writing – review & editing, Writing – original draft, Visualization, Validation, Supervision, Project administration, Methodology, Investigation, Formal analysis, Conceptualization. **Jun Yang:** Supervision, Project administration, Funding acquisition, Formal analysis. **Xuhong Qian:** Supervision, Methodology, Investigation.

Acknowledgments

This work is supported by grants from National Key R&D Program of China (Nos. 2024YFC2511100 and 2024YFC2511105 to J. Yang), National Natural Science Foundation of China (Nos. 82230035 and 82271179 to J. Yang, 82000977 and 82371150 to S. Hou, 82000989 to P. Chen), and Shanghai Sailing Program (Nos. 20YF1428800 to P. Chen, 20YF1428900 to S. Hou).

Supplementary materials

Supplementary material associated with this article can be found, in the online version, at doi:10.1016/j.cclet.2025.111447.

References

[1] S. Champlin, S. Miller, A. Griffith, et al., Health. Commun. 40 (2024) 848–855.
[2] W.J.T. Tan, L. Song, Hear. Res. 434 (2023) 108783.
[3] G.E. Gregory, K.J. Munro, K.N. Couper, et al., Clin. Immunol. 249 (2023) 109287.
[4] T. Zou, R. Xie, S. Huang, et al., Biochem. Pharmacol. 222 (2024) 116115.
[5] Y. Wang, K. Hirose, M.C. Liberman, J. Assoc. Res. Otolaryngol. 3 (2002) 248–268.
[6] S.M. Vlajkovic, P.R. Thorne, Int. J. Mol. Sci. 22 (2021) 5647.
[7] M. Teraoka, N. Hato, H. Inufusa, et al., Int. J. Mol Sci. 25 (2024) 4146.
[8] Y. Zhou, C. Fang, L. Yuan, et al., J. Otolaryngol. Head Neck Surg. 52 (2023) 78.
[9] J.S. Kempfle, D.H. Jung, Expert. Opin. Investig. Drugs 32 (2023) 643–654.
[10] K. Xu, B. Xu, J. Gu, X, et al., Theranostics 13 (2023) 3524–3549.
[11] A. Pisani, F. Paciello, R. Montuoro, et al., Life 13 (2023) 1035.
[12] J.T. Sanchez, S. Ghelani, M.S. Otto, Neuroscience 285 (2015) 248–259.
[13] C.G. Le Prell, J. Am. Acad. Audiol. 32 (2021) 670–694.
[14] J. Hu, Y. Fang, X. Huang, et al., Adv. Drug Deliv. Rev. 179 (2021) 114005.
[15] Y. Huang, J. Ren, X. Qu, Chem. Rev. 119 (2019) 4357–4412.
[16] Z. Sun, J. Huang, Z. Fishelson, et al., Biomedicines 11 (2023) 1971.
[17] D. Raucher, S. Dragojevic, J. Ryu, Front. Oncol. 8 (2018) 624.
[18] H. Oliveira, C. Sao-Jose, J. Azeredo, Viruses 10 (2018) 292.
[19] L. Zhao, Y. Zhang, Y. Yang, et al., Chem. Asian J. 17 (2022) e202200573.
[20] C. Dai, L. Wang, X. You, et al., Chin. Chem. Lett. 36 (2025) 109869.
[21] L. Zhang, L. Lei, Z. Zhao, et al., Chin. Chem. Lett. 36 (2025) 110316.
[22] Y. Wang, H. Fu, B. Huang, et al., Chin. J. Eng. 479 (2024) 155684.
[23] S. Liu, R. Yang, Front. Neurosci. 16 (2022) 867453.
[24] V.A. Petrova, A.A. Panevin, S.G. Zhuravskii, et al., Int. J. Biol. Macromol. 120 (2018) 1023–1029.
[25] H. Zhang, H. Chen, L. Lu, et al., Adv. Sci. 11 (2024) e2305215.
[26] S. Dash, J. Zuo, P.S. Steyger, Pharmaceuticals 15 (2022) 1115.
[27] R.A. Dop, D.R. Neill, T. Hasell, ACS Appl. Mater. Interfaces 15 (2023) 20822–20832.
[28] A.K. Blakney, P.F. McKay, K. Hu, et al., J. Control. Release 338 (2021) 201–210.
[29] C. Viegas, F. Seck, P. Fonte, J. Drug Deliv. Sci. Technol. 77 (2022) 103839.
[30] A. Fu, R. Tang, J. Hardie, M.E. Farkas, Bioconjug. Chem. 25 (2014) 1602–1608.
[31] J. Buse, A. El-Aneed, Nanomedicine 5 (2010) 1237–1260.
[32] P. Wen, H. Huang, R. Zhang, et al., Nat. Chem. 17 (2025) 279–288.
[33] T. Liang, Y. Dong, I. Cheng, et al., Nat. Biomed. Eng. 8 (2024) 1469–1482.
[34] C. Forenzo, J. Larsen, Mol. Pharm. 20 (2023) 4387–4403.
[35] Y. Sun, X. Xu, L. Chen, et al., ACS Nano 17 (2023) 16597–16606.
[36] Y. Sun, S.Y. Lau, Z.W. Lim, et al., Nat. Chem. 14 (2022) 274–283.
[37] L. Zhou, H. Shi, Z. Li, Macromol. Rapid. Commun. 41 (2020) e2000149.
[38] M. Abbas, J.O. Law, S.N. Grellscheid, et al., Adv. Mater. 34 (2022) e2202913.
[39] M. Abbas, W.P. Lipiński, J. Wang, et al., Chem. Soc. Rev. 50 (2021) 3690–3705.
[40] T. Lu, X. Hu, M.H.I. van Haren, et al., Small 19 (2023) e2303138.
[41] B. Wang, H. Fang, W. Zhu, et al., ACS Appl. Mater. Interfaces 14 (2022) 36998–37008.
[42] S. Nayak, K. Das, S. Sivagnanam, et al., iScience 27 (2024) 109523.
[43] M.S.A. Abdelaty, Polym. Bull. 80 (2023) 5759–5783.
[44] T.Y. Duan, H.B. Li, Biomacromolecules 21 (2020) 2258–2267.
[45] Y. Chen, M. Yuan, Y. Zhang, et al., Biomater. Sci. 10 (2022) 4588–4595.
[46] Y. Chen, M. Yuan, Y. Zhang, et al., Chem. Sci. 11 (2020) 8617–8625.
[47] S. Liu, Y. Zhang, M. Li, et al., Nat. Chem. 12 (2020) 1165–1173.
[48] Y. Zhang, S. Liu, Y. Yao, et al., Small 16 (2020) e2002073.
[49] J. Liu, L. Tian, Y. Qiao, et al., Angew. Chem. Int. Ed. 59 (2020) 6853–6859.
[50] S. Chen, F. Yang, Z. Zhu, et al., Vet. Microbiol. 274 (2022) 109550.
[51] J.L. Larabee, G.D. Hauck, J.D. Ballard, J. Biol. Chem. 293 (2018) 1810–1819.
[52] H.J. Eom, J. Choi, Chem. Biol. Interact. 311 (2019) 108774.
[53] R. Li, C. Chen, S. Zhu, et al., Biochem. J. 476 (2019) 483–497.
[54] F. Wu, K. Hill, Q. Fang, et al., Cell Mol. Life Sci. 79 (2022) 249.
[55] S. Early, E. Du, E. Boussaty, et al., Hear. Res. 425 (2022) 108505.
[56] O. Akil, S.L. Rouse, D.K. Chan, et al., J. Vis. Exp. 97 (2015) 52187.
[57] J. Zhang, T. Gong, P. Chen, et al., Free Radic. Biol. Med. 225 (2024) 641–653.
[58] Z. Guo, Y. Wu, B. Chen, et al., Natl. Sci. Rev. 11 (2024) nwae100.
[59] X. Huang, X. Kou, T. Zhan, et al., Stem Cell Res. Ther. 14 (2023) 88.
[60] X. Min, X.H. Deng, H. Lao, et al., J. Control. Release 364 (2023) 546–561.
[61] H. Xiong, L. Lai, Y. Ye, Neurosci. Bull. 37 (2021) 657–668.
[62] A.R. Fetoni, F. Paciello, R. Rolesi, et al., Free Radic. Biol. Med. 135 (2019) 46–59.
[63] E.M. McElnea, E. Hughes, A. McGoldrick, et al., BMC Ophthalmol. 14 (2014) 153.
[64] S. Hou, P. Chen, J. He, et al., Redox Biol. 57 (2022) 102472.
[65] A.R. Fetoni, V. Zorzi, F. Paciello, et al., Redox Biol. 19 (2018) 301–317.
[66] S. Gao, T. Nie, L. Jiang, et al., Mater. Today Bio 27 (2024) 101141.
[67] L. Wang, R. Zhang, L. Jiang, et al., Biomater. Sci. 12 (2024) 4006–4023.